ISSN 0006-3509, Biophysics, 2008, Vol. 53, No. 2, pp. 140–146. © Pleiades Publishing, Inc., 2008.
Original Russian Text © I.B. Kovalenko, A.M. Abaturova, P.A. Gromov, D.M. Ustinin, G.Yu. Riznichenko, E.A. Grachev, A.B. Rubin, 2008, published in Biofizika, 2008, Vol. 53, No. 2, pp. 261–270.

CELL BIOPHYSICS

# Computer Simulation of Plastocyanin–Cytochrome *f* Complex Formation in the Thylakoid Lumen

**I. B. Kovalenko[a], A. M. Abaturova[a], P. A. Gromov[b], D. M. Ustinin[a], G. Yu. Riznichenko[a], E. A. Grachev[b], and A. B. Rubin[a]**

[a] *Biological Faculty, Moscow State University, Moscow, 119992 Russia*
[b] *Physical Faculty, Moscow State University, Moscow, 119992 Russia*
*e-mail: kovalenko78@mail.ru*

Received June 13, 2007; in final form, September 17, 2007

**Abstract**—Plastocyanin diffusion in the thylakoid lumen and its binding to cytochrome *f* (a subunit of the membrane $b_6f$ complex) were studied with a direct multiparticle simulation model that could also take account of their electrostatic interaction. Experimental data were used to estimate the model parameters for plastocyanin–cytochrome *f* complexing in solution. The model was then employed to assess the dependence of the association rate constant on the dimensions of the lumen. Highest rates were obtained at a lumen span of 8–10 nm; narrowing of the lumen below 7 nm resulted in drastic deceleration of complexing. This corresponded to the experimentally observed effect of hyperosmotic stress on the interaction between plastocyanin and cytochrome *f* in thylakoids.

*Key words:* plastocyanin, cytochrome *f*, diffusion, electron carriers, electrostatic interaction, direct simulation modeling

**DOI:** 10.1134/S0006350908020048

## INTRODUCTION

In higher plants and algae, photosystems (PS) I and II use the absorbed light energy to initiate the photosynthetic electron and proton transport in the thylakoid. The cytochrome $b_6f$ complex couples the two systems, accepting electrons from PS II and passing them to PS I. The latter step is executed by the mobile electron carrier plastocyanin (Pc).

This small (10.5 kDa) protein diffuses in the lumen, a relatively narrow closed space between the thylakoid membranes, oxidizing cytochrome *f* (Cyt*f*) in the membrane complex and then reducing the PS I reaction center. In the process it travels for quite large distances (hundreds of nanometers), shuttling between the granal and stromal regions of the thylakoid [1, 2].

In a native chloroplast, the span of the lumen (4–10 nm [3]) is commensurate with the Pc dimensions ($40 \times 28 \times 30$ Å, Fig. 1). Therefore, Pc diffusion in the lumen is perhaps substantially hindered by the protruding parts of transmembrane oligoenzyme complexes and by other mobile molecules [4]. Electrostatic interactions are known to play a key role in Pc binding to the membrane complexes at physiological ionic strength, pH, and temperature. The interplay of electrostatic attraction and repulsion forces provides for directed movement of Pc to the binding site, and the molecule is orientated in the electric field of the complex [4].

The width of the lumen may change upon osmotic stress as well as upon variations of illumination and pH (e.g. [5]). A recent review [6] lists averaged distances between two neighboring membrane pairs in the granal stacks, obtained by analysis of electron micrographs from 17 literature sources. Taking the thickness of one membrane to be about 5 nm, we can calculate from these data that the span of the lumen ranges from 4 to 14 nm, with values of 6 and 11 nm being most common. The lumen in granal stacks was reported to decrease by one-third upon illumination [5], so these values may correspond to the states of light and dark adaptation. Recently [7] electron microscopic tomography has been used to reconstruct the three-dimensional organization of thylakoid membranes in higher plant chloroplasts. The mean thickness of the granal layer, i.e., two membranes and the lumenal space between them, has been estimated at $20 \pm 2$ nm, which corresponds to a mean lumenal span of 10 nm.

Assessments of the influence of hyperosmotic stress on thylakoids [8, 9] showed opposite effects on Pc interaction with P700 and Cyt*f*; this apparent discrepancy will be discussed later.

The lateral distribution of Pc was examined by immunocytochemical location and the redox kinetics of $P700^+$ [10]. Upon dark adaptation, the Pc concentration

*Abbreviations:* Cyt*f*, cytochrome *f*; Pc, plastocyanin; PS, photosystem.

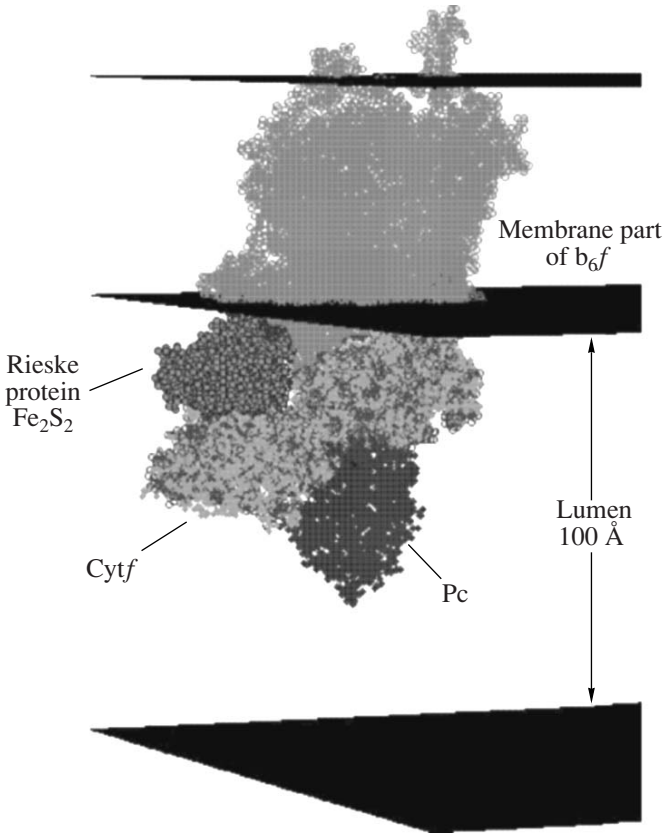


**Fig. 1.** The arrangement of the Pc–Cyt*f* complex on the membrane-embedded $b_6$ *f*, obtained by combining the PDB structures 2PCF and 1Q90.

in the stromal region of the lumen proved to be about twice that in the granal region. Illumination caused a Pc concentration rise in the granal region and a decline in the stromal region, and it was concluded that light induces Pc migration. A portion of Pc entering the granal region may "stick" to the membrane because of lowered pH. Since light also causes shrinking of the granal lumen, some Pc molecules may be immobilized, which would attenuate the electron flow from the cytochrome complex to PS I in the granal regions.

To study Pc diffusion in the lumen and its interaction with the membrane complexes, it is expedient to build a model that would take into consideration, on the one hand, the restrictive geometry of the lumenal space and, on the other hand, the influence of electrostatic interactions between the electron carrier proteins. Over the last decade, Brownian dynamics has been employed to assess the kinetic characteristics of complex formation between two proteins. Thus interaction of Pc and Cyt*f* was modeled in solution, the complexing process was analyzed, the structure of the protein complex was examined, and the possibility of electron transfer therein was evaluated [11–14]. However, these works did not consider the diffusion of Pc molecules in the thylakoid lumen or their interaction with the $b_6f$ and PS I membrane-bound complexes.

In our previous work [15] we developed a method for direct computer simulation of diffusion and interaction of mobile electron carrier proteins that takes account of the geometry of the reaction volume and of the carriers. In a more recent study [16] we simulated the complexing of Pc and Cyt*f* in solution with allowance for their shapes and electrostatic interactions. The dependences of the rate constant on ionic strength were generated for wild-type Pc and seven mutant forms, and comparison with the experimental data testified to the validity of our description.

Here we use direct computer simulation to study the formation of the Pc–Cyt*f* complex in the thylakoid. In the model, membranes delimit the lumenal space, the Cyt*f* particles are exposed into the lumen in accordance with the experimental evidence on $b_6f$ structure and arrangement, while Pc diffuses in the lumen. In this way we have obtained the dependence of the association rate constant on the geometry (length and width) of the lumenal space and the disposition of the membrane complexes.

## MODEL DESCRIPTION

### The Model Stage

Figure 2 shows the reaction volume modeling the lumenal space as a rectangular parallelepiped; from the top and bottom it is delimited by membranes, mirror boundary conditions are applied at the butts. The membrane area, the intermembrane distance, the density of membrane-bound complexes, and the concentrations of mobile carriers were estimated from the literature data.

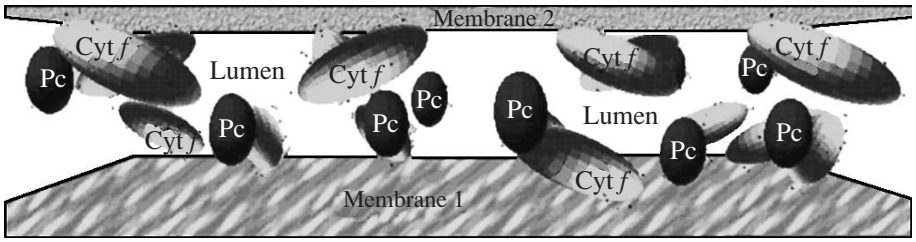


**Fig. 2.** The model stage with plastocyanin (Pc) in the lumen and Cyt*f* bound to thylakoid membranes (hatched).

Thus the diameter of the granal membrane is 300–600 nm [17], the $b_6f$ density on the membrane is 2.55 per 1000 nm$^2$ [18], [Pc] = 430 μM.

The $b_6/f$ complex of *Chlamydomonas reinhardtii* comprises four large subunits—Cyt*f*, Cyt$b_6$, Rieske iron-sulfur protein, and subunit IV—and four small hydrophobic subunits [19]. The Rieske protein and Cyt*f* extend into the lumen (Fig. 1). The Pc diffusing in the lumen forms a complex with Cyt*f* to oxidize it. An NMR structure of a complex between spinach Pc and turnip Cyt*f* was obtained in 1998 ([20], PDB code 2PCF). In 2003, an X-ray structure was established for *C. reinhardtii* $b_6f$ (1Q90). Combining these structures, we found the possible mutual positions of Pc and Cyt*f* relative to the membrane (Fig. 1) and used this arrangement in modeling. It is taken that Pc molecules diffusing in the lumen can make a complex with immobile Cyt*f* partners only upon assuming the appropriate orientation.

## Protein Movement and Interaction

Interaction of mobile electron carrier proteins can be conventionally divided into several steps [2]: (i) diffusion and approach owing to mutual electrostatic attraction; (ii) interaction between parts of molecules, mutual orientation in space and formation of a preliminary complex; (iii) conformational rearrangements in proteins and establishment of a transfer-competent complex; and (iv) electron transfer within this complex. Our model explicitly describes diffusion, electrostatic interaction and pre-complexing. Conformational changes, hydrophobic and van der Waals interactions are taken in implicitly through the docking probability parameter.

The method of modeling the Pc–Cyt*f* interaction in solution is described elsewhere [16]. Here the same method is applied to simulate the process in the narrow membrane-limited lumen. Since every molecule is considered as a separate object in a 3D space of finite volume and definite shape, the modeling in a limited lumenal space has no basic differences from that in solution. The only distinction is the denser positioning of molecules in space and the possibility of collisions of the Pc particles with the membrane ("walls" of the reaction volume), which is naturally and easily accommodated in modeling the particle motion. The Pc molecules are regarded as Brownian particles undergoing translational and rotational motions in a viscous medium under the action of a random force (arising from collisions with molecules of the milieu) and an electrostatic force. We make use of the Langevin equation describing the time change in every coordinate caused by these forces.

For the translational motion the equation appears as

$$\xi_{\mathrm{tr}}^{x}\frac{dx}{dt} = f_x(t) + F_x$$

where $x$ is the corresponding coordinate, $\xi_{\mathrm{tr}}^{x}$ is the coefficient of viscous friction along this coordinate, $f_x(t)$ and $F_x$ are the projections of the random and the electrostatic forces on the $x$ axis. The random force has a normal distribution with zero mean and variance $\frac{2kT\xi_{\mathrm{tr}}^{x}}{\Delta t}$, where $k$ is the Boltzmann constant and $T$ is temperature.

For the rotational motion we have

$$\xi_{\mathrm{rot}}^{x}\frac{d\varphi}{dt} = m_x(t) + M_x$$

where $\xi_{\mathrm{rot}}^{x}$ is the friction coefficient for rotation about the $x$ axis, $m_x(t)$ and $M_x$ are the moments of the random and the electrostatic forces relative to the $x$ axis.

To simplify the calculation of friction coefficients, the Pc and Cyt*f* molecules were represented as ellipsoids of rotation. The 3D model of the molecule was constructed from the PDB data. The ellipsoid size and axes were chosen so that the rotational moment of inertia was minimal and the moments of inertia of the initial molecule and the corresponding ellipsoid coincided under uniform potential density.

The model stage is described by setting an orthogonal coordinate system. Mirror boundary conditions are imposed at the edges. Every object of the model stage (i.e., mobile carrier) is assigned its own (intrinsic) coordinate system aligned with the axes of the ellipsoid; such a system is chosen because the friction coefficients for the ellipsoid are known.

The Langevin equation is solved numerically in these intrinsic orthogonal coordinates: the displacements of the ellipsoid along and rotations about its axes under the action of Brownian force are calculated at every step. These values are then recalculated into translations and rotations in the stage coordinates. The position of every object in the model is defined by the displacement and rotation matrix of the intrinsic versus stage coordinate systems.

To calculate protein collisions, their shapes were described with sets of spheres. To verify a collision, it was necessary to check whether the corresponding sets intersect. The radii and center coordinates of the spheres were chosen so that with a minimal set of spheres the deviation of the resulting shape from the protein surface did not exceed 2 Å.

Special attention is paid to electrostatic interactions between the proteins, which are known to be very important for Pc–Cyt*f* binding [2, 4, 21]. The charged amino acid residues create a nonuniform electric field around the protein molecule. If the given protein is remote from other objects, its movement is determined solely by free Brownian diffusion. Approaching other proteins (complexes), it orientates in their electric field and may assume a position favorable for subsequent binding.

Our model considers a protein as a region with a dielectric constant ε = 2 and spatially distributed fixed charges [22]. The solution is a region of ε = 80 with mobile charges (ions). At large distances between protein particles, the electrostatic interactions are very weak because of field screening by water molecules; therefore, in the model they are admitted only when the protein surfaces approach within 35 Å, called the electrostatic interaction distance. At this distance, screening in a solution of ionic strength corresponding to 100 mM diminishes the electrostatic potential by a factor of 80 as compared with a salt-free solution [22].

For each kind of protein, the electric field potential is calculated within a certain area around the molecule. To find the force (and its moment) acting on a particular charge in the protein, we calculate the potential gradient created in this point by other proteins. The force and moment for the protein molecule as a whole are obtained by summation over all its charges.

### *Model Parameters*

Chaotic Brownian motion in the model can cause approach of two or more proteins within the electrostatic interaction distance. Therewith the proteins orienting in the electric field of other proteins can take a binding-favorable position and form a preliminary complex. The latter means that that the distance between the interacting sites of the molecules is smaller than a certain value we call the docking distance, which is a model parameter (Table 1). The subsequent processes leading to the final complex are implicit in the parameter of docking probability. Opportune choice of these parameters ensures the preferred mutual orientation of the proteins.

Thus the docking distances $r_i$ are the distances between certain residues of Pc and Cyt*f* in complex. Binding of proteins in appropriate mutual orientation takes place with a certain probability *P* called docking probability.

At each step, the sum amount of reduced and oxidized molecules of Pc and Cyt*f* is calculated, and these data are then used to plot the kinetic curves for the redox states. Approximating such a curve in accordance with the law of mass action, we can obtain the rate constant for the second-order reaction of Pc–Cyt*f* binding.

We have previously [16] estimated the model parameters (docking distance and probability) at which the rate constants calculated as above for wild-type and mutant Pc's at 100 mM ionic strength were most close to the experimental values [23]. These parameters were determined as follows. The docking distances were taken as those between the atoms of Pc and Cyt*f* residues that are immediate neighbors in the complex [20] and between the Cu and Fe atoms. For different combinations of docking distances (varied from 10 to 50 Å in 1-Å steps) we obtained the dependences of the association rate constant on docking probability for wild-type and seven mutant Pc's.

**Table 1.** Atom–atom distances in the Pc–Cyt*f* complex used as conditions for complexing in the simulation

| Pc and Cyt*f* residues neighboring in complex | Atom numbers and names | | Distance in the model, *R*, Å |
|---|---|---|---|
| | Pc | Cyt*f* | |
| D42-R209 | 591 – OD2 | 3278 – HH2 | 18 |
| E43-K187 | 607 – HB | 2930 – HE | 18 |
| D44-K185 | 618 – OD2 | 2895 – HZ | 18 |
| E60-K58 | 842 – HA | 912 – HZ | 25 |
| – | 1435 – Cu | 3881 – Fe | 40 |

**Table 2.** Pc–Cyt*f* reaction rate constants at 100 mM ionic strength, determined experimentally [23] for Pc wild type (wt) and specified mutants at pH 6 and those obtained by modeling with docking distances from Table 1 and docking probability of 0.01

| Protein | $k_2$, $10^6$ $M^{-1}$ $s^{-1}$ (expt) | $k_c$, $10^6$ $M^{-1}$ $s^{-1}$ (model) |
|---|---|---|
| wt | 185 (±20) | 159 (±4) |
| Q88E | 220 (±30) | 287 (±9) |
| D42N | 76.5 (±1.5) | 76 (±3) |
| E43N | 56.1 (±1) | 73 (±3) |
| E43K | 29.3 (±0.7) | 36.9 (±0.5) |
| E43Q/D44N | 26.9 (±0.6) | 23.9 (±0.7) |
| E59K/E60Q | 13.8 (±0.2) | 23.9 (±0.8) |
| E59K/E60Q/E43N | 5.56 (±0.01) | 8.2 (±0.8) |

It turned out that to uniquely define the Pc position relative to Cyt*f*, it is sufficient to set the distances in five atomic pairs (Table 1). Our rate constants best fitted the experiment at a docking probability of 0.01 (Table 2). The qualitative correspondence thus observed suggests that the proposed method of direct modeling is applicable to Pc–Cyt*f* interaction in solution.

Hereafter we use the above-specified parameters to model the complexing of Pc with Cyt*f* in the thylakoid lumen, supposing that these elementary characteristics of protein–protein interaction do not depend on the volume and dimensions of the system.

## RESULTS

Using computer simulation, we modeled the step of complexing between Pc and Cyt*f*; the electron transfer within the resulting complex was taken to be comparatively rapid [4].

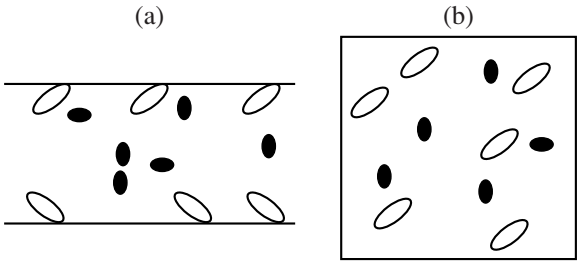


**Fig. 3.** Two stage versions for numerical experiments: (a) Cyt*f* molecules are membrane-bound in accordance with structural data; (b) all molecules diffuse in a cubic space of the same volume as in (a).

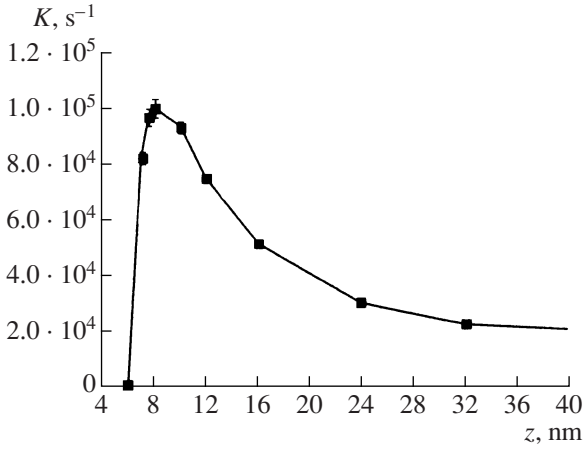


**Fig. 4.** The rate of Pc–Cyt*f* complexing normalized to Cyt*f* concentration in the thylakoid versus the intermembrane distance $z$ (at a constant number of molecules).

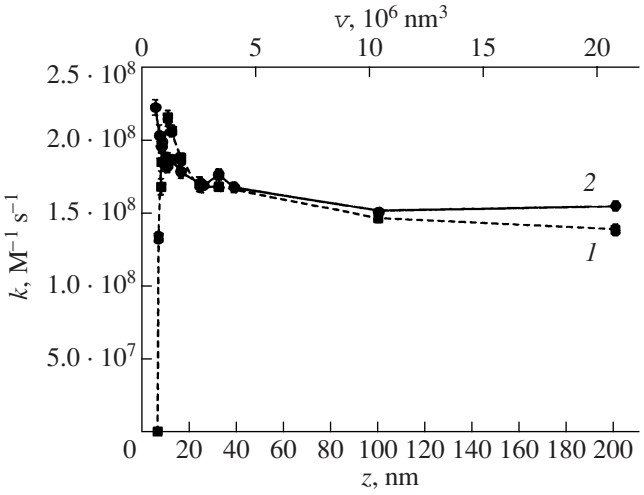


**Fig. 5.** The bimolecular reaction rate constant for Pc–Cyt*f* complexing as a function of (*1*) intermembrane distance $z$ in the thylakoid and (*2*) volume $v$ of a cubic space for diffusion. The number of molecules is constant and the same in both cases.

The dependence of the rate of Pc–Cyt*f* complexing in the thylakoid on lumen width (distance between membranes) was assessed by varying the latter from 200 to 7 nm but keeping constant the number of molecules (270 each) and the membrane area ($322 \times 322$ nm). We considered two cases (Fig. 3) with the Cyt*f* molecules (a) membrane-bound and exposed in the lumen and (b) diffusing together with Pc in a cubic space of the same volume. Case (a) corresponds to the experimental data on Cyt*f* disposition in the thylakoid, case (b) corresponds to the experiment with isolated particles in solution. The results of numerical simulation are displayed in Figs. 4 and 5.

As follows from Fig. 4, the association rate is highest at a lumen width of 8 nm; it declines at larger widths because of the decrease in effective Pc concentration, but is also lower at smaller widths.

Likewise, Fig. 5 shows that the second-order rate constant is maximal ($k = 2.2 \cdot 10^8$ $M^{-1}$ $s^{-1}$) at the intermembrane distance $z$ of 8–10 nm (curve *1*, case (a) in Fig. 3). At $z < 7$ nm the rate constant abruptly drops to zero. Indeed, Cyt*f* with attached Pc protrude from the membrane to 7 nm, so if the opposite membrane is closer than this, the complex cannot be formed. With increasing $z$ the rate constant also decreases, probably because at the initial moment the Pc molecules prove to be farther away from the membrane-bound Cyt*f*. When both Pc and Cyt*f* diffuse in a cubic space (case (b) in Fig. 3, curve *2* in Fig. 5), the rate constant does not drop at small reaction volumes. One can also see that $k$ does not appreciably change at $v > 5 \cdot 10^6$ $nm^3$ or $z > 40$ nm.

We approximated the curve obtained for the solution in accordance with the law of mass action implying equiprobable collisions of molecules throughout the reaction time. Initially the reagents are well mixed, the molecules occupy random positions but no two particles are within the interaction distance. In an ideal solution, the second-order rate constant should not depend on concentration changes. At the initial moment, however, the rate "constant" is very high owing to pairs of relatively close molecules (probably aided by electrostatic interactions), but then $k$ declines to a steady-state value [24] observed in the experiment.

We also examined how the rate of Pc–Cyt*f* complexing in the thylakoid depends on the lateral dimension of the lumen at its constant width of 10 nm and constant number of molecules (270 each). Curve *1* in Fig. 6 corresponds to case (a) in Fig. 3. Thus the lumen was a square parallelepiped with base side $x$ varied from 200 to 1200 nm. For comparison, we plotted the data (curve *2*) for the equivalent cubic volume of solution (case (b) in Fig. 3).

It is clear that the rate constant rises with decreasing reaction volume. This means that the law of mass action is disobeyed at high concentrations. Note that for the membrane-bound case the rate is always higher than for the solution case. Most probably, the membranes confine the Pc diffusion and prevent its leaving the attrac-

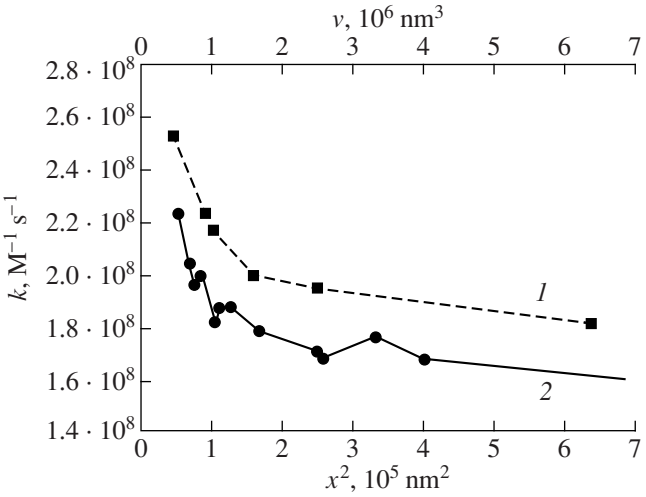


**Fig. 6.** The bimolecular reaction rate constant for Pc–Cyt*f* complexing as a function of (*1*) area $x^2$ of the 10-nm lumen and (*2*) volume $v$ of a cubic space for diffusion. The number of molecules is constant and the same in both cases.

tion area of Cyt*f* particles bound in the interaction-prone orientation.

## DISCUSSION

The results of direct simulation demonstrate the dependence of the rate of Pc–Cyt*f* complexing in the thylakoid on the span of the lumen. The interaction is suppressed when the lumen is narrowed to 7 nm, because the complex simply does not have enough space to form.

It has been reported [8] that in *C. reinhardtii* thylakoids under hyperosmotic stress the lumen loses water and shrinks on average from 5 to 1.5 nm, and this inhibits Pc interactions with Cyt*f* and P700; indeed, Pc is 2.8 nm in the smallest dimension. We think that the lumen width in [8] was underestimated, as compared with the data from a literature survey [6] and 3D reconstruction [7] and considering that the pressure exerted in preparing chloroplast thin sections could have caused compression. In contrast, an earlier work [9] with isolated higher plant thylakoids reported that hyperosmotic stress increased the rate of Pc interaction with Cyt*f* and P700; this was explained by a higher Pc concentration in the smaller lumenal space. Apart from technicalities, this discrepancy might be due to that the thylakoid membrane interfaces in *Chlamydomonas* and higher plants differ also in their ability to prevent the collapse of the lumen. However, our simulation data can largely reconcile these observations. For instance, reading Fig. 4 from right to left, we see an appreciable rise in the interaction rate as the lumen narrows to ~8 nm but a steep drop to zero upon further contraction. The opposite effects in [8, 9] may correspond to the opposite slopes of such a dependence.

The interaction between Pc and the $b_6/f$ complex in the thylakoid is an example of a biochemical reaction that can be modulated by changes in the physical characteristics of the surroundings, in this case the lumen span. We suppose that such events are physiologically relevant and expedient: adjustment of the electron transport at the plastocyanin level by narrowing the lumen, together with checking the proton release into the lumen upon plastoquinol interaction with the cytochrome complex and other mechanisms, would prevent photoinduced damage under intense illumination and attenuate the linear electron transport [25]. This is quite in accord with the already mentioned data (e.g. [5]) on light-driven constriction of the lumen. Notably, this physical mechanism is operative in the granal regions and affects the linear electron transport, while the stroma lamellae where the cyclic electron transport takes place exhibit no changes in lumen width or the rate of electron transfer from Cyt*f* to Pc.

## REFERENCES

1. A. B. Hope, Biochim. Biophys. Acta **1143**, 1 (1993).
2. E. L. Gross, in *Oxygenic Photosynthesis: The Light Reactions,* Ed. by D. R. Ort and N F. Yocum (Kluwer Acad. Publ., Dordrecht, 1996), pp. 413-429.
3. M. Menta, V. Sarafis, and C. Critchley, Aust. J. Piant Physiol. **26**, 709 (1999).
4. A. B. Hope, Biochim. Biophys. Acta **1456**, 5 (2000).
5. S. Murakami and L. Packer, J. Cell Biol. **47**, 332 (1970).
6. J. P. Dekker and E. J. Boekema, Biochim. Biophys. Acta **1706**, 12 (2005).
7. E. Shimoni, O. Rav-Hon, J. Ohad, et al., Plant Cell **17**, 2580 (2005).
8. J. A. Cruz, B. A. Salbilla, A. Kanazava, and D. M. Kramer, Plant Physiol. **127**, 1167 (2001).
9. W. Haehnel, A. Propper, and H. Krause, Biochim. Biophys. Acta **593**, 384 (1980).
10. W. Haehnel, R. Ratajczak, and H. Robenek, J. Cell Biol. **108**, 1397 (1989).
11. G. M. Ullmann, E.-W. Knapp, and N. M. Kostic, J. Am. Chem. Soc. **119**, 42 (1997).
12. D. C. Pearson Jr. and E. L. Gross, Biophys. J. **75**, 2698 (1998).
13. F. Rienzo, R. Gabdoulline, M. Menziani, et al., Biophys. J. **81**, 3090 (2001).
14. E. L. Gross and D. C. Pearson Jr., Biophys. J. **85**, 2055 (2003).
15. I. B. Kovalenko, D. M. Ustinin, N. E. Grachev, et al., Biofizika **48**, 656 (2003).
16. I. B. Kovalenko, A. M. Abaturova, P. A. Gromov, et al., Phys. Biol. **3**, 121 (2006).
17. L. A. Staehelin G. W. M. van der Staay, in *Oxygenic Photosynthesis. The Light Reactions,* Ed. by D. R. Ort and

C. F. Yocum (Kluwer Academic Publishers, 1996), pp. 11–30.

18. P.-A. Albertsson, Trends in Plant Science **6** (8), 349 (2003).
19. D. Stroebel, Y. Choquet, J.-L. Popot, and D. Picot, Nature **426**, 413 (2003).
20. M. Ubbink, M. Ejdebeck, B. G. Karlsson, and D. S. Bendall, Structure **6**, 323 (1998).
21. C. Kieanthous, *Protein-Protein Recognition* (Oxford University Press, New York, 2000).
22. A. V. Finkelstein and O. B. Ptitsyn, *Protein Physics* (KD Universitet, Moscow, 2002) [in Russian].
23. A. Kaant, S. Young, and D. S. Bendall, Biochim. Biophys. Acta **1277**, 115 (1996).
24. A. Kh. Vorob'ev, *Diffusion Problems in Chemical Kinetics* (Izd. MGU, Moscow, 2003) [in Russian].
25. A. B. Rubin, *Biophysics* (KD Universitet, Moscow, 2000) [in Russian].